

Received January 9, 2020, accepted March 2, 2020, date of publication March 11, 2020, date of current version March 24, 2020.

Digital Object Identifier 10.1109/ACCESS.2020.2980188

An Improved Kinematic Model Predictive Control for High-Speed Path Tracking of Autonomous Vehicles

LUQI TANG^{1,2,3}, FUWU YAN^{1,2,3}, BIN ZOU^{1,2,3}, KEWEI WANG^{1,2,3},
AND CHEN LV⁴, (Member, IEEE)

¹Hubei Key Laboratory of Advanced Technology for Automotive Components, Wuhan University of Technology, Wuhan 430070, China

²Hubei Collaborative Innovation Center for Automotive Components Technology, Wuhan University of Technology, Wuhan 430070, China

³Hubei Research Center for New Energy & Intelligent Connected Vehicle, Wuhan 430070, China

⁴School of Mechanical and Aerospace Engineering, Nanyang Technological University, Singapore 639798

Corresponding author: Bin Zou (zoubin@whut.edu.cn)

This work was supported in part by the National Natural Science Foundation of China under Grant 51975434, in part by the Overseas Expertise Introduction Project for Discipline Innovation under Grant B17034, in part by the Innovative Research Team in University of Ministry of Education of China under Grant IRT_17R83, and in part by the Department of Science and Technology, Hubei Provincial People's Government under Grant 2019AEA169.

ABSTRACT Kinematic model predictive control (MPC) is well known for its simplicity and computational efficiency for path tracking of autonomous vehicles, however, it merely works well at low speed. In addition, earlier studies have demonstrated that tracking accuracy is improved by the feedback of yaw rate, as it improves the system transients. With this in mind, it is expected that the performance of path tracking can be improved by a cascaded controller that utilizes kinematic MPC to determine desired yaw rate rather than steering angle, and uses proportional-integral-derivative (PID) control to follow the reference yaw rate. However, directly combining MPC with PID feedback control of yaw rate results in a controller with poor tracking accuracy. The simulation results show that the cascaded MPC-PID controller has relatively stable but larger error compared to classic kinematic and dynamic MPC. Based on the analysis of vehicle sideslip angle, a novel path tracking control method is proposed, which is designed using a kinematic MPC to handle the disturbances on road curvature, a PID feedback control of yaw rate to reject uncertainties and modeling errors, and a vehicle sideslip angle compensator to correct the kinematic model prediction. The proposed controller performances involving steady-state and transient response, robustness, and computing efficiency were evaluated on Carsim/Matlab joint simulation environment. Furthermore, field experiments were conducted to validate the robustness against sensor disturbances and time lag. The results demonstrate that the developed vehicle sideslip compensator is sufficient to capture steer dynamics, and the developed controller significantly improves the performance of path tracking and follows the desired path very well, ranging from low speed to high speed even at the limits of handling.

INDEX TERMS Autonomous vehicles, path tracking, lateral control, model predictive control.

I. INTRODUCTION

In recent years, research on autonomous vehicles has seen great achievement together with computer and sensors technology advances. As one of major components in autonomous vehicles, path tracking aims at following a desired path or trajectory via controlling the vehicle in lateral and longitudinal motion. In general, this reference path is generated by path planning module. Due to the nonlinearity

of the vehicle dynamics, time lag, uncertainties, and road curvature disturbances, ensuring tracking accuracy and vehicle stability simultaneously is considered to be a great challenge [1], [2]. The ideal path tracking controller should take into account future road information and be capable of rejecting disturbances and parameter uncertainties.

To date, extensive research on path tracking has been carried out and usually involves in feedforward-feedback or optimization control. Early tracking controllers are mostly developed based on geometric vehicle model and feedback control theory due to its simplicity and stability,

The associate editor coordinating the review of this manuscript and approving it for publication was Jenny Mahoney.

namely, the deviation inputs of the feedback controller are obtained by the geometrical relationship between vehicle and road. For instance, in the studies [3]–[5], different proportional-integral-derivative (PID) control architectures are proposed to follow the given path. Pure pursuit method, as a standard benchmark, has been widely used in several DARPA Challenge vehicles [6]. These methods are simple but merely work well in a narrow operating window, since these controllers always calculate errors at one or several preview points and are unable to capture complete steer dynamics. To improve these methods, many adaptive approaches that automatically tune look-ahead distance depending on curvature and speed have been proposed [7]–[9].

More recently, with the advances of computer performance, model predictive control (MPC) has been shown to be an attractive control algorithm for path tracking problem [9]–[12]. It has the advantage of handling the constraints on the state variables and control inputs and achieving multi-objective optimization, such as driver comfort, time consumption, tracking accuracy. For instance, Wang *et al.* proposed an improved MPC controller based on fuzzy adaptive control to improve both tracking accuracy and ride comfort which can adjust the weights of cost function adaptively based on lateral position error and heading error [13]. Aiming at the tracking error representation, Sun *et al.* believed that path tracking accuracy and vehicle stability can hardly be accomplished by one fixed control frame in various conditions. Then, the authors presented a novel MPC controller with switched tracking error which mainly involves different treatments regarding sideslip angle in computing the heading deviation [14].

Inspired by more precise modeling, actuator dynamics is incorporated to capture the transient response of the vehicle into collision avoidance constraints [15]. Cai *et al.* presented a MPC controller using a 4-DOF vehicle model to reflect the characteristics of vehicle dynamics to avoid rollover accidents of automobiles [16]. In addition, considering the noise in the localization and planning stage, a model-based linear quadratic gaussian control with adaptive Q-matrix was proposed to tracking controller design [17]. Although MPC method with prediction has the ability to forecast future dynamic behaviors and significantly improves path tracking, it requires solving optimization problem repeatedly at each control step. This may lead to heavy computational burden and potential risks in real-time implementation. Moreover, many vehicle parameters play an important role in vehicle dynamic, however, these parameters probably change over time, such as vehicle mass and cornering stiffness [18]. Actually, it should be noted that it is very difficult to accurately characterize the nonlinearities by existing several semi-empirical tire model [19]. Therefore, pure MPC method may be unsatisfactory in real applications when taking into account computational efficiency and prediction accuracy at the same time.

To reject the aforementioned uncertainties and disturbances, many classical control theories are also explored,

such as fuzzy control [20], sliding mode control [2]. These types of classical control deal with worst-case disturbances, which often lead to too conservative performance [21]. In addition, these feedback control methods rely on system instantaneous states and usually are incapable of predicting future behaviors. Consequently, this drawback results in the lack of flexibility of road curvature disturbances. Recently, due to advances in hardware, sensors and artificial intelligence, large amounts of data can be collected. Data-driven methods attract increasing attention in the field of autonomous driving. For instance, NVIDIA trained a convolutional neural network to map raw pixels from a single front-facing camera directly to steering commands, which is well-known as end-to-end approach [22]. Nitin *et al.* investigated the path tracking of racecar via iterative learning control in consideration of the nonlinear vehicle dynamics and unmodelled road conditions during racing task [23]. Shida *et al.* proposed a data-driven method, model-free adaptive control for the lateral motion of an autonomous vehicle [24]. The major drawback of these approaches is the huge amount of training data set representing various driving situations, which makes data-driven methods have not yet applied to the real world as successfully as MPC techniques.

In summary, the path tracking controller need to have the ability to handle the road curvature disturbances with prediction, reject uncertainties using feedback control, and become high efficient in computation. With this in mind, in this paper, a new path tracking control architecture is proposed, which is designed using a MPC controller based on vehicle kinematics to handle the disturbances on road curvature, a PID feedback control of yaw rate to reject uncertainties and modeling errors, and a vehicle sideslip angle compensator to correct the above prediction process.

Although it is well known that kinematic vehicle model is unsuitable for high-speed path tracking as they are inaccurate in regions of tire force saturation [25], the proposed controller based on kinematic model follows the desired path very well, ranging from low speed to high speed even at the limits of handling. This is mainly caused by the involvements of these aforementioned two elements, i.e., the feedback control of yaw rate and vehicle sideslip compensation. It has been demonstrated in earlier studies that the tracking accuracy is improved by additional feedback of the yaw rate which can be measured by a gyro, as it improves the system transients, by changing the eigenvalues displacement of the steering dynamics [2], [4], [26]. Consequently, the main contributions of this paper are as follows.

- 1) To handle the challenges of path tracking at high speed and sharp curves, a novel tracking control architecture is developed, consisting of three main components: kinematic model predictive control, feedback control of yaw rate, and vehicle sideslip compensation.

- 2) A vehicle sideslip angle compensator is utilized to correct the prediction process using kinematic model, which is designed based on the relationship between sideslip and yaw

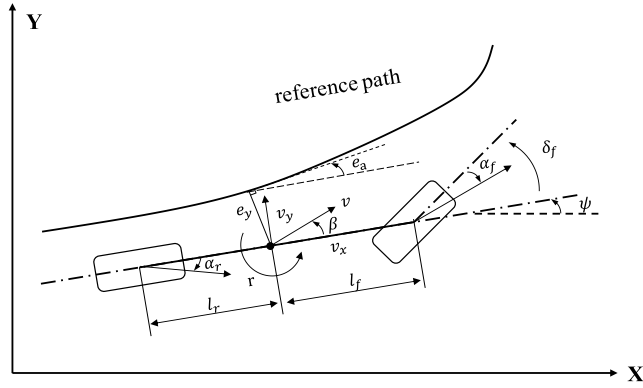


FIGURE 1. Kinematic bicycle model where α_f and α_r denote the front and rear wheel slip angles, respectively. r is yaw rate.

rate, and formulized as an expression involving yaw rate and current vehicle speed.

The remainder of this paper is organized as follows: Section II presents the vehicle lateral kinematic and dynamic model; and Section III introduces the lateral control design for path tracking; Section IV evaluates the proposed control method and compares it with classic kinematic and dynamic MPC; and the field test is presented in Section V. Section VI concludes this paper.

II. MODELING

In this section, kinematic bicycle modeling and dynamic modeling are carried out respectively. The kinematic model is the basis of the proposed control design and used to predictive control, however, the dynamic model is explored to understand steer dynamics and contribute to vehicle sideslip compensator design.

A. KINEMATIC BICYCLE MODEL

The kinematic bicycle model is given by the following set of equations in an inertial frame according to the axes system with SAE standards [19] (see Figure 1), under the assumptions: 1) The vehicle is assumed to have planar motion, and the vertical, pitch and roll motions are ignored; 2) The slip angles at both wheels are zero.

$$\dot{X} = v \cos(\psi + \beta) \tag{1a}$$

$$\dot{Y} = v \sin(\psi + \beta) \tag{1b}$$

$$\dot{\psi} = \frac{v \cos(\beta)}{l_f + l_r} (\tan(\delta_f) - \tan(\delta_r)) \tag{1c}$$

$$\beta = \tan^{-1} \left(\frac{l_f \tan(\delta_r) + l_r \tan(\delta_f)}{l_f + l_r} \right) \tag{1d}$$

where X denotes global X axis coordinate, Y global axis coordinate, v the speed of the vehicle, ψ the heading angle of the vehicle, β vehicle sideslip angle, l_f and l_r represent the distance from the center of the mass of the vehicle to the front and rear axles, respectively. δ_f and δ_r are the steering angles for the front and rear wheels. we assume $\delta_r = 0$, as in most vehicles the rear wheels cannot be steered.

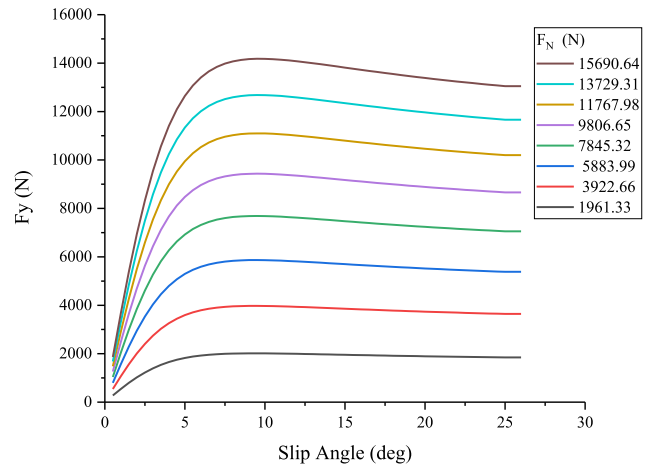


FIGURE 2. Absolute lateral tire force as a function of slip angle, with different vertical tire load F_N .

In this paper, the path tracking control aims at minimizing the lateral and heading deviation of the autonomous vehicle with respect to a given reference path at arbitrary safe speed ranging from low speed to extremely high speed at the limits of handling. Figure 1 illustrates the schematic diagram of path tracking model which demonstrates the geometric relationships between autonomous vehicle and the desired lane. e_a denotes the heading deviation that is the orientation error between the heading of vehicle and the tangential direction of the road centerline. e_y denotes the lateral deviation that is the distance of the c.g. of the vehicle from the center line of the lane.

Generally, the kinematic bicycle model described above is suitable for control law design at low speed. However, at high-speed scenarios, this prediction model will become increasingly unreliable, due to the rise of tire sideslip angles. Therefore, it is necessary to investigate the vehicle dynamics and tire side-slip characteristics for improving the controller performance.

B. TIRE and VEHICLE DYNAMIC MODEL

It is well known that tire force plays a key role in the analysis of vehicle motion, as in addition to aerodynamic forces and gravity, all the forces that affect vehicle motion are produced by the tires. To some extent, due to the complexity of tire model, obtaining vehicle models of sufficient accuracy is not available in real time. Moreover, it is very difficult to precisely formulate the nonlinearities by a unified tire force model. Most of the existing tire models are predominantly “semi-empirical” in nature, such as Burckhardt model, Magic formula, and Dugoff model [19]. These semi-empirical tire models involve severe nonlinearities as shown in Figure 2, resulting in many difficulties in stability analysis and real-time controller design [20]. Nevertheless, the typical tire model shown in Figure 2 also indicates that in normal driving situations where the slip angles are small, the relation between lateral force and slip angle is nearly linear. Under

such assumption, the tire model can be characterized by a simplified linear model that the lateral tire forces are approximately linear with respect to the tire slips and given as

$$F_{yf} = C_f \alpha_f \quad (2)$$

$$F_{yr} = C_r \alpha_r \quad (3)$$

where F_{yf} and F_{yr} are the lateral tire force of the front and rear wheels, respectively, α_f and α_r denote the front and rear wheel slip angles, respectively, C_f and C_r denote the front and rear wheel cornering stiffness, respectively. The tire slip angles α_f and α_r can be expressed as

$$\alpha_f = \beta + \frac{l_f \dot{\psi}}{v} - \delta_f \quad (4)$$

$$\alpha_r = \beta - \frac{l_r \dot{\psi}}{v} \quad (5)$$

With the aforementioned linear tire model and certain assumptions: 1) Ignoring the weight transfers and road bank angle, the left and right tire sideslip angles on the same axle are identical; 2) The roll and pitch dynamics are neglected, the vehicle lateral dynamic model can be expressed as [2], [27]

$$\ddot{x} = \dot{\psi} \dot{y} + a_x \quad (6a)$$

$$\ddot{y} = -\dot{\psi} \dot{x} + \frac{2}{m} (F_{yf} \cos(\delta_f) + F_{yr}) \quad (6b)$$

$$\ddot{\psi} = \frac{2}{I_z} (l_f F_{yf} - l_r F_{yr}) \quad (6c)$$

$$\dot{X} = \dot{x} \cos(\psi) - \dot{y} \sin(\psi) \quad (6d)$$

$$\dot{Y} = \dot{x} \sin(\psi) + \dot{y} \cos(\psi) \quad (6e)$$

where a_x is longitudinal acceleration, m denotes vehicle mass, I_z is yaw moment of inertia.

It can be seen from the comparison between kinematic and dynamic model that although the kinematic model also involves vehicle sideslip angle β , it assumes that all tire slip angles are deemed to be zero which will lead to significant model mismatch as tire slip angles increase, such as at high speed scenarios. This drawback of kinematic model motivates the proposed vehicle sideslip compensator which is one of our main contributions.

The main vehicle parameters are summarized in Table 1 and the tire cornering stiffness is determined by the tire model depicted in Figure 2 that the lateral tire forces are calculated as a function of vertical load, lateral tire slip angle. The source data in Figure 2 is from Carsim software by setting the type of tires as “225/60 R18”.

III. CONTROLLER DESIGN

As mentioned above, the objective of path tracking control is to keep the vehicle as close as possible to the given path under the desired speed. In this paper, we decouple the problems of path tracking into lateral control design and longitudinal control design, which is similar to many previous work [28], [29]. Additionally, we only focus on the lateral control under the assumptions that the given path and desired

TABLE 1. Vehicle parameters.

Parameter	Symbol	Value	Units
Vehicle mass	m	1650	kg
Yaw inertia	I_z	3234	kg·m ²
Front axle to CG	l_f	1.65	m
Rear axle to CG	l_r	1.4	m

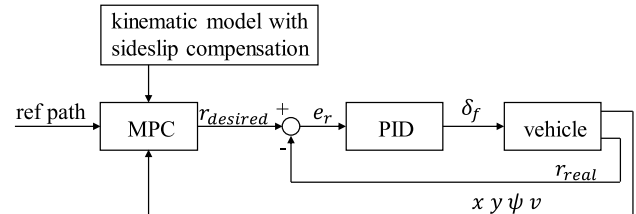


FIGURE 3. Lateral control scheme where $r^{desired}$, r^{real} denote the desired and real yaw rate, respectively. e_r is the error between the desired and real yaw rate.

speed are obtained from existing modules. Therefore, the steering angles of front wheels δ_f is the only output of the proposed controller.

In this section, a novel lateral control scheme is proposed, which is the main contribution of our work. The proposed control scheme is illustrated in Figure 3. It is designed as a hybrid MPC-PID cascade control loop. The external control loop produces the yaw rate reference signal using a kinematic MPC controller with vehicle sideslip compensation. Compared to the PID control in Marino’s work [4], the MPC control law has considerable advantage on rejecting the disturbances on road curvature and velocity variation, with the ability to predict future behaviors of vehicle. The inner PID control loop is to track rapidly the yaw rate reference coming from the external one. As mentioned in introduction, this design based on yaw rate is inspired by the existing studies that additional feedback of the yaw rate leads to a significant reduction of tracking error in nearly all driving maneuvers, as it improves the system transients [2], [4], [26].

A. CASCADED MPC-PID CONTROL

Model predictive control has been widely used in the field of path tracking, in general, which can be roughly classified into two methods: kinematic MPC and dynamic MPC, depending on the vehicle model [30]. Each method has its own pros and cons. kinematic MPC is simple, but only works well at low speed. As speed increases, the kinematic model mismatch will result in large tracking error. On the contrary, dynamic MPC can overcome the impact of increasing speed, however, it has the drawback of poor computational efficiency and becomes singular at low vehicle speeds, no matter linear dynamic model or nonlinear model.

To deal with the above dilemma, we explore a cascaded kinematic MPC-PID controller in this section, with the expectation that PID feedback control of yaw rate is capable

of rejecting uncertainties and modeling errors, meanwhile, the controller retains superior computational efficiency. Considering the fact that the output of predicting model is yaw rate rather than the steering angles of front wheels δ_f , the δ_f needs to be eliminated from (1c), (1d). Substituting from (1c) into (1d), the vehicle sideslip angle β can be rewritten as

$$\beta = \sin^{-1} \left(\frac{l_r}{v} \dot{\psi} \right) \quad (7)$$

Then, substituting from (7) into (1a), (1b), the kinematic model used in MPC can be rewritten as

$$\dot{X} = v \cos \left(\psi + \sin^{-1} \left(\frac{l_r}{v} \dot{\psi} \right) \right) \quad (8a)$$

$$\dot{Y} = v \sin \left(\psi + \sin^{-1} \left(\frac{l_r}{v} \dot{\psi} \right) \right) \quad (8b)$$

$$\dot{\psi} = r \quad (8c)$$

where yaw rate r is the output of MPC controller and yaw rate reference tracked by the PID inner loop via controlling the steering angles of front wheels.

Based on the kinematic model (8), the desired yaw rate is obtained by a typical MPC module. We used the publicly available solver IPOPT [31] to solve the following optimization problem. At each time, the following constrained finite horizon optimal control problem is solved:

$$\begin{aligned} \min_u \quad & \sum_{i=1}^{H_p} (z_i - z_{ref,i})^T Q (z_i - z_{ref,i}) \\ & + \sum_{i=0}^{H_c-1} \left[(u_i - u_{i-1})^T M (u_i - u_{i-1}) + u_i^T R u_i \right] \\ \text{s.t.} \quad & z_0 = z(t), u_{-1} = u(t - t_s) \\ & z_{i+1} = f(z_i, u_i), i = 0, \dots, H_p - 1 \\ & r_{\min,i} \leq u_i \leq r_{\max,i}, \quad \forall i \\ & \Delta r_{\min,i} \leq u_i - u_{i-1} \leq \Delta r_{\max,i}, \quad \forall i \end{aligned} \quad (9)$$

where, as in standard MPC notation, Q , M and R are weighting matrices of appropriate dimensions. The reference signal z_{ref} represents the desired output, where $z = [\psi, Y]^T$. H_p , H_c denote the prediction horizon and control horizon, respectively. Time t_s is the sampling time of the path tracking controller. $f(z_i, u_i)$ denotes the state update with the kinematic model derived in (8) through forward Euler. In particular, if $f(z_i, u_i)$ update with the kinematic model (1) or the dynamic model (6), we will achieve classic kinematic MPC and dynamic MPC controllers, respectively [30]. The variables $r_{\min,i}$, $r_{\max,i}$, $\Delta r_{\min,i}$, $\Delta r_{\max,i}$ denote lower and upper bounds of the yaw rate and the constraints on increment of yaw rate, respectively. $u_{t,i} = [u_t, \dots, u_{t+H_c-1}]$ is the optimization vector at time t . Especially, u_{-1} represents the control action at the previous sampling step and the first value $u_{t,0}$ of the optimization vector is used as the optimal control action:

$$r_{desired} = u_{t,0} \quad (10)$$

where $r_{desired}$ is the MPC controller output, namely, the yaw rate reference tracked by PID controller of the inner loop.

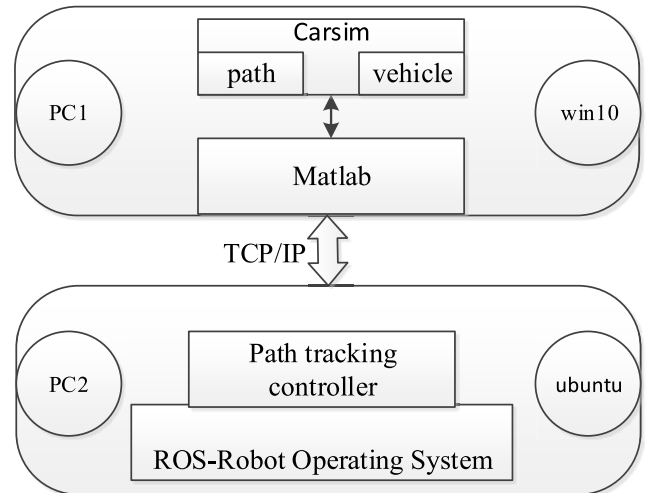


FIGURE 4. Simulation system architecture.

Once the MPC control loop is designed, the remaining step is to design the PID inner loop controller. The goal of the PID controller is to minimize the yaw rate error e_r between the measured yaw rate r_{real} and desired yaw rate $r_{desired}$. The relationship between the error e_r and output δ_f can be formulated in the following standard PID control law,

$$e_r = r_{desired} - r_{real} \quad (11)$$

$$\delta_f = K_p e_r(t) + K_i \int_0^t e_r(t) dt + K_d \frac{de_r(t)}{dt} \quad (12)$$

with proportional, integral and differential gain K_p , K_i , K_d .

It should be noted that yaw rate would not change with steering angles δ_f at a standstill, which can also be derived by equation (1c). Therefore, this cascaded MPC-PID control method is not appropriate for stop-and-go scenarios and automatic parking, if K_i is not set to zero.

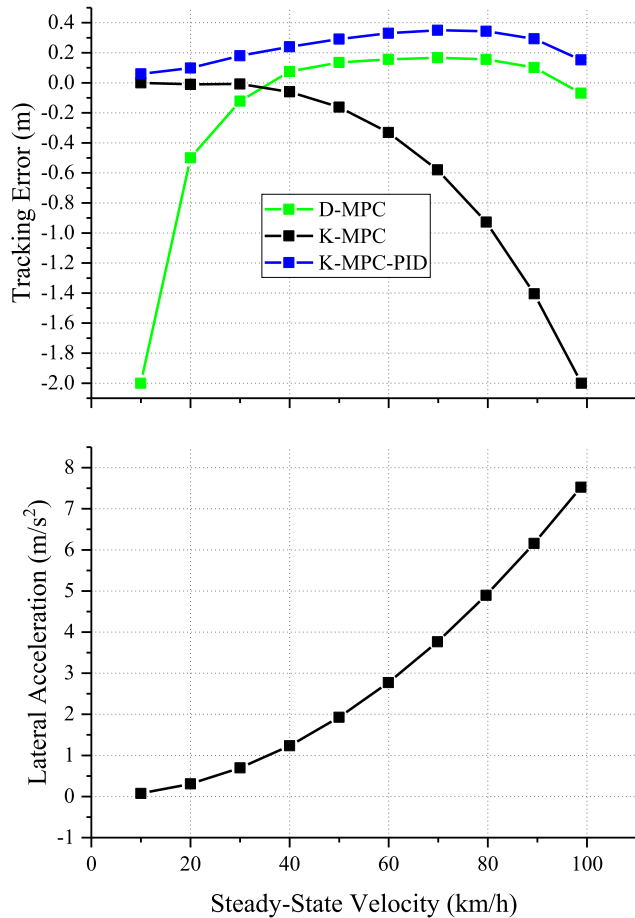
B. STEADY-STATE RESPONSE with MPC-PID CONTROL

In order to test the above MPC-PID control law, we implemented the MPC controller in C++ and evaluated it on Carsim/Matlab joint simulation environment. An overview of the simulation system architecture is outlined in Figure 4. The simulation system is composed of two personal computers. One is used for the path tracking controller based on Ubuntu OS and Robot Operating System with an intel i5-4590 processor. The other one aims at providing a simulator involving path and autonomous vehicle based on Carsim/Matlab. Carsim, as a high-fidelity vehicle simulator, utilizes detailed nonlinear tire models and vehicle models to simulate the dynamic behaviors of different types of vehicle and is widely used in automotive industry [20]. The TCP/IP networking protocol is used to communicate between the above two computers. Table 2 lists the main controller parameters which are the same for all controllers presented in this paper.

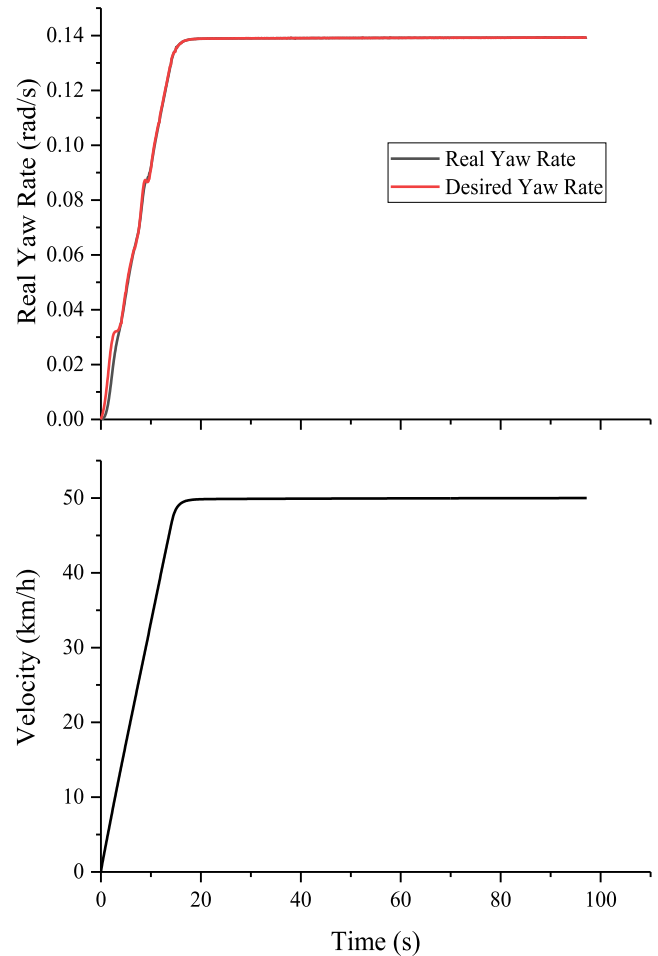
Figure 5 shows the steady-state responses of three types of controllers for following a circular path with a radius of 100m as a function of vehicle speed. These controllers

TABLE 2. Main controller parameters.

Parameter	Symbol	Value	Units
prediction horizon	H_p	10	-
control horizon	H_c	10	-
sampling time	t_s	0.1	s

**FIGURE 5.** Steady-state response for following a circular path with a radius of 100m. Each simulation test indicated by dots on the corresponding curve was implemented at constant vehicle speed, ranging from 10 to 100 in intervals of 10 km/h.

are classic kinematic MPC, dynamic MPC and MPC-PID control law, based on kinematic model (1), dynamic model (6) and the modified kinematic model (8), respectively. It is apparent that reaching a certain point, the lateral tracking errors grow with the vehicle speed under the classic kinematic MPC control, on the contrary, if the speed is decreased to a certain point, the tracking errors will be increased for dynamic MPC. The point of intersection of the above two curves is close to 35 km/h. This confirms the expected results from the consensus in existing literature that kinematic model is unsuitable for high-speed path tracking, and the dynamic MPC control becomes singular at low vehicle speeds [25], [30]. Moreover, it is of interest to note that directly combining MPC with PID feedback control of yaw

**FIGURE 6.** The performance of PID control for tracking the desired yaw rate.

rate results in a controller with poor tracking accuracy. The cascaded MPC-PID control law never obtains the lowest tracking error no matter how fast the vehicle moves, compared to the other two MPC control methods. However, the cascaded MPC-PID controller still makes a difference in path tracking that the tracking error is relatively stable and is limited into a range of 0.4 m without excessive deviation from the desired path, which demonstrates the contribution of the feedback of yaw rate and also implies some systematic bias.

To further find out the reason for the poor accuracy of MPC-PID controller, the performance of PID control for tracking the desired yaw rate is illustrated in Figure 6 which is extracted from one of the above steady-state tests under the control of MPC-PID controller. The results show that the inner PID control loop follows the desired yaw rate very well when the vehicle speed is held at 50 km/h. Therefore, there must be some significant model mismatch in the external MPC control loop and the desired yaw rate generated via the kinematic model (8) needs to be corrected. With this in mind, a compensation for vehicle sideslip is proposed to alleviate the above model mismatch and improve tracking accuracy under MPC-PID control law.

C. COMPENSATION FOR VEHICLE SIDESLIP

The classic kinematic model (1) and the derived kinematic model (8) both involve the vehicle sideslip angle β , however, it should be noted that obtaining the vehicle sideslip angle β in both model are under the assumptions that the slip angles at both wheels are zero. As it is shown in (4), (5), there exists direct correlation among β and the tire slip angles α_f, α_r . Therefore, in high-speed scenarios, these assumptions will lead to severe mismatch between predicting model and vehicle dynamics inevitably. In this section, a more accurate form of vehicle sideslip angle β is derived from steady-state cornering conditions with linear tire model. First, at steady-state conditions (road curvature rate $\dot{k} = 0, \dot{v} = 0$), the rear tire forces can be given by the following simplified equation as described by Kapania et al. [1].

$$F_{yr} = \frac{ml_f}{l_f + l_r} v^2 k \tag{13}$$

Then, substituting from (13) and linear tire model (3) into (5), yields the vehicle sideslip angle:

$$\beta = \frac{ml_f}{(l_f + l_r)C_r} v^2 k + \frac{l_r \dot{\psi}}{v} \tag{14}$$

Since road curvature $k = \frac{1}{R} = \frac{\dot{\psi}}{v}$, the proposed sideslip compensator can be obtained by rewritten (14) as

$$\beta = \frac{ml_f}{(l_f + l_r)C_r} v \dot{\psi} + \frac{l_r \dot{\psi}}{v} \tag{15}$$

where yaw rate $\dot{\psi}$ is the output of the proposed MPC control loop. Therefore, at each prediction stage of solving the MPC problem, the predicted sideslip angle β will update with $\dot{\psi}$. Then substituting from (15) into (1a), (1b), yields the kinematic model:

$$\dot{X} = v \cos(\psi + \beta) \tag{16a}$$

$$\dot{Y} = v \sin(\psi + \beta) \tag{16b}$$

$$\beta = K_1 v \dot{\psi} + K_2 \frac{\dot{\psi}}{v} \tag{16c}$$

$$\dot{\psi} = r \tag{16d}$$

where $K_1 = \frac{ml_f}{(l_f + l_r)C_r}, K_2 = l_r$. In practice, parameters K_1, K_2 can be empirically tuned through simulation or field test, and their effects are further explored in Section IV. Note that the sideslip compensator will become singular at a standstill because of the denominator involving the velocity v . To avoid this situation, the velocity v will be replaced by a threshold when the vehicle starts at a standstill. Replacing kinematic model (8) with kinematic model (16) under the framework of cascaded MPC-PID control, we obtain the proposed controller.

IV. CONTROLLER PERFORMANCE

To better understand the performance of the proposed control law, in this section we analyze system steady-state and transient responses, the effect of the parameters K_1, K_2 , the robustness against measurement error and parameters uncertainties, and computing efficiency.

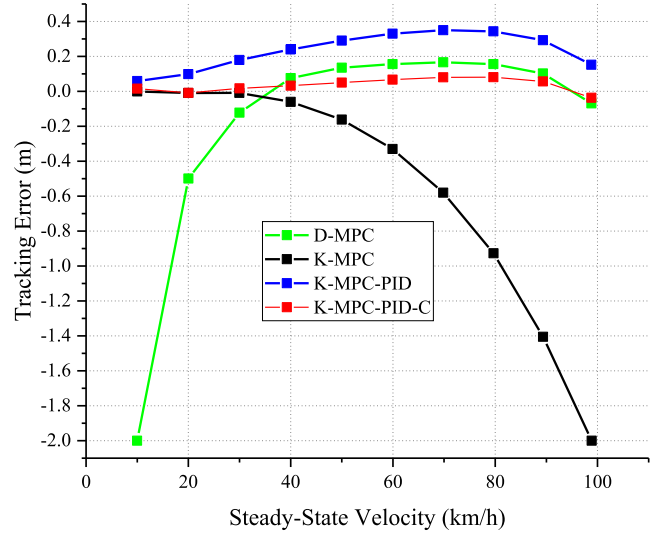


FIGURE 7. Steady-state response with sideslip compensation.

A. STEADY-STATE RESPONSE

Figure 7 demonstrates the steady-state response of the designed MPC-PID control law with sideslip compensation (K-MPC-PID-C). The simulation setting is consistent with that in Figure 5. The results show the excellent performance of the proposed controller that outperforms all the other controllers in this steady-state test. First, at low speed both classic kinematic MPC and our controller follow the desired path well, however, as vehicle speed increases the classic kinematic MPC becomes unacceptable, but the tracking error of the proposed control law is immune to increasing. Second, the proposed control law is superior to both dynamic MPC and MPC-PID without compensation throughout the whole range of vehicle speed. Third, at both low speed and high speed, even at the limits of handling, the maximum of lateral errors under sideslip compensation are less than 0.1 m.

B. TRANSIENT RESPONSE

Figure 8 shows the transient state responses for tracking a sinusoidal path with an amplitude of 4m and a wavelength of 50 m, mimicking the lane-change maneuver. The results indicate that all controllers have the similar tracking performance as the steady-state tests and the designed controller still follows the sinusoidal path well throughout the whole range of vehicle speed, despite approaching the limits of handling with the maximum lateral acceleration of 8.4 m/s². This figure also illustrates that although the classic kinematic MPC achieves the best tracking accuracy when speed is lower than 30 km/h, the maximum tracking errors of the proposed controller also have not exceed a limit of 0.1 m. Then, as speed increases, the designed controller becomes the only available control law in this test with maximum error of 0.16 m. In addition, one can observe that the dynamic MPC is not capable of following the desired path at high lateral acceleration conditions as the steady-state test in Figure 7, despite the fact that the vehicle reaches to a similarly high

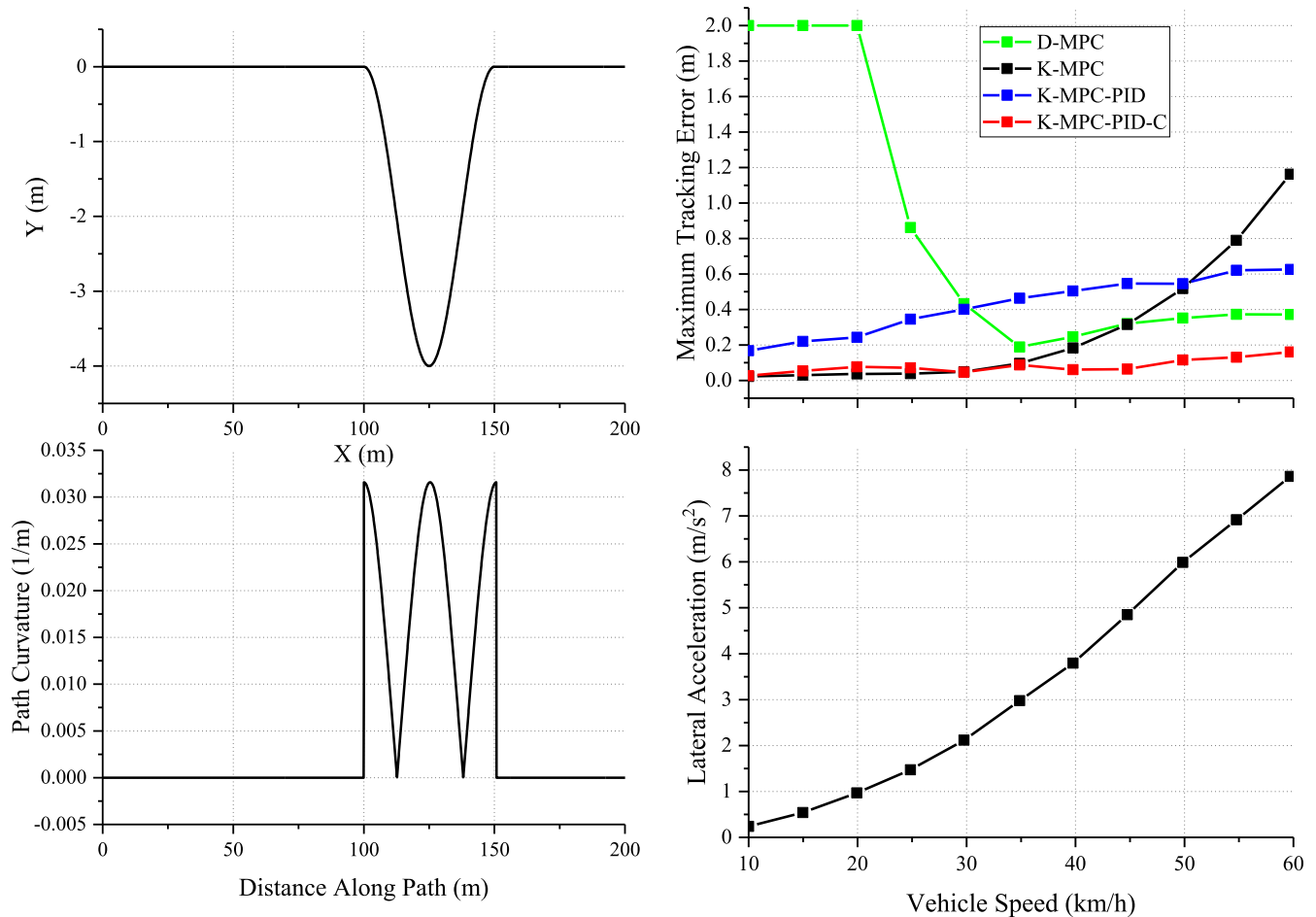


FIGURE 8. Transient state responses as a function of vehicle speed for following a sinusoidal trajectory $Y = 2 \sin\left(\frac{2\pi}{T}\left(x + \frac{1}{4}\right)\right) - 2, T = 50$. Each simulation test indicated by dots on the corresponding curve was implemented at constant vehicle speed, ranging from 10 to 60 in intervals of 5 km/h.

level of speed (beyond 40 km/h). The reason for this is that the tire dynamics become so difficult to model at the limits of handling where the mismatch of linear dynamic model is unable to be neglected anymore. It is apparent that this drawback makes it difficult to combine the kinematic MPC and dynamic MPC, that is, the controller cannot trigger a switch from kinematic MPC to dynamic MPC just according to the increase of vehicle speed, because their tracking performances depend on not only vehicle speed, but also road curvature and the resulting lateral acceleration. The above weakness of classic MPC for path tracking highlights the contribution of the proposed control law that with the derived sideslip compensation, the cascaded MPC-PID control achieves exact tracking accuracy from low speed to high speed with different road curvature.

C. EFFECT of the PARAMETERS K_1, K_2

Parameters K_1, K_2 derived from the sideslip compensator (15) and (16c) have their own theoretical definition, but in practice we may be unable to obtain the precise value of those related parameters such as vehicle mass and tire cornering stiffness. Therefore, for a better sense of the effect of the parameters K_1, K_2 in sideslip compensator, Figure 9 shows the changing

trend of the lateral tracking error for the designed controller at varying group of the parameters K_1, K_2 by steady-state test. The results reveal a tradeoff in tuning K_1 and K_2 . When K_1 is set to zero, the larger K_2 is capable of providing the better tracking accuracy at low speed, but the worse tracking accuracy at high speed. Then, when K_2 is set to a proper constant, K_1 has the ability to improve the tracking accuracy at high speed while ensure the tracking performance at low speed. It can be see that the maximum of lateral error takes place at the speed of around 80 km/h with the coupling effect of K_1 and K_2 , rather than the top speed of 100 km/h at the limits of handling. Consequently, this coupling effect could be used to tune the two parameters K_1 and K_2 for the best tracking performance in accordance with the highest design speed. In addition, the designed sideslip compensator could be also incorporated into those advanced online estimations on tire cornering stiffness [32] and vehicle mass [33] for further improvement in path tracking.

D. ROBUSTNESS

In essence, the designed control law is a cascaded MPC-PID control that the inner PID feedback control loop struggles to track rapidly the desired yaw rate produced by the MPC

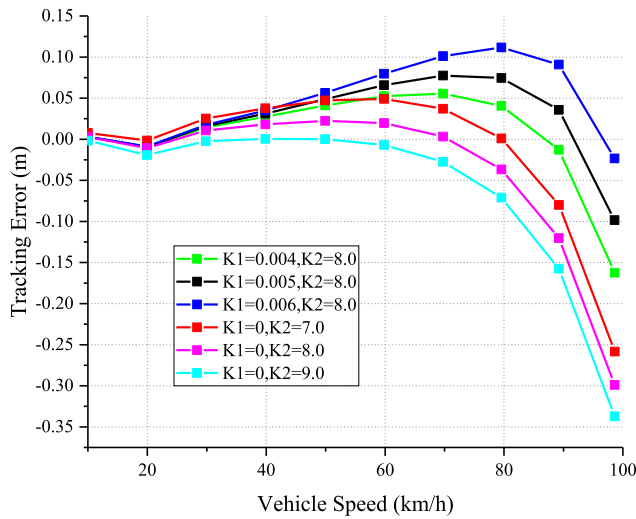


FIGURE 9. The effect of the parameters K_1 , K_2 in sideslip compensator.

loop. Therefore, the measurement of yaw rate plays a key role in this approach compared to other path tracking methods. For this reason, the robustness of the proposed controller performance with respect to the measurement error of the yaw rate sensor is tested in steady-state and transient scenarios near the limits of handling. In addition, the robustness against parameters uncertainties regarding the vehicle mass and tire cornering stiffness are also validated with simulation, because the derived kinematic model (16) with sideslip compensation is related to both of them.

Controller robustness against measurement error of the yaw rate sensor:

The measurement error of the yaw rate is modeled as Gaussian distribution with a Matlab block called Random Number and injected to the original yaw rate calculated by the Carsim vehicle model. In field test presented in Section V, the yaw rate is measured by the inertial navigation system RT3002 which measures the yaw rate at the error level of $0.01^\circ/\text{s}$, 1σ . Then, the disturbance of measurement error is set to two orders of magnitude higher than that in the sensor specification, i.e., $1^\circ/\text{s}$. Moreover, in the transient test, we add the case that measurement error mean or variance is $10^\circ/\text{s}$ to explore where the tracking performance will get worse, although the measurement accuracy of real sensors will not be so inferior. As shown in Figure 10, the results of steady and transient tests show that if the measurement error is within the range that both the mean and variance are less than $1^\circ/\text{s}$, the tracking performance of the proposed controller is not significantly affected by the disturbance of measurement error and controller achieves the equivalent tracking accuracy compared to the cases of no noises. As the level of disturbance further increases, the actual tracking path has gradually deviated from the desired path as shown in Figure 10 (b). The tracking error is approximately 0.5m when mean of measurement error is $10^\circ/\text{s}$ and variance is $1^\circ/\text{s}$. However, the $0.01^\circ/\text{s}$ angular rate accuracy with sensor RT3002 is far better than the above error of $1^\circ/\text{s}$ and once control system

is successful to be deployed, the mean of measurement error can be eliminated by control parameter tuning. Therefore, the simulation results prove that the controller is capable of following the path with the measurement error of yaw rate sensors, which is further validated in field test presented in next section.

Controller robustness against parameters uncertainties:

The robustness of the controller is evaluated over vehicle parameters uncertainty with respect to vehicle mass and tire cornering stiffness. Figure 11 shows the steady-state and transient responses where payloads of four passengers with different mass are set in Carsim to simulate the effect of mass uncertainties. The steady-state tracking error increases as payload increases, especially at high speed, however, all tracking trajectory in transient responses nearly coincide with each other even at the limits of handling where the resulting peak lateral acceleration is 8.6 m/s^2 . This interesting observation is consistent with the mathematical derivation of sideslip compensator (15) and (16c) that only gain K_1 involves the term mass and the product of K_1 and vehicle speed is used to compensate the sideslip dynamics. Thus, The robustness against vehicle mass decreases as speed increases. Nevertheless, the designed controller is still able to meet the demand of path tracking with acceptable errors despite the variations of vehicle mass, as shown in Figure 11.

As for tire cornering stiffness, there are more complicated responses than that of vehicle mass variations. First, Figure 12 shows that when the cornering stiffness drops 25 percent or more, the vehicle will slide off the road at the limits of handling because the tires are incapable of producing adequate lateral forces. Second, it can be observed that the controller has the ability to reject uncertainties that cornering stiffness has increased by 25%, however, as it further climbs, the tracking error is beyond 0.2 m indicating that the controller fails to follow the desired path. Like the impact of vehicle mass, the cornering stiffness variations impose stronger disturbances at high speed than low speed with similarly high level of resulting lateral acceleration.

E. COMPUTING EFFICIENCY

Figure 13 shows the comparison for computational cost of three types of MPC controller for path tracking. we implemented all these MPC controllers in C++ with solver IPOPT on Linux system with an intel i5-4590 processor. Moreover, the same MPC parameter configurations are set to ensure a fair comparison that both the prediction horizon and control horizon are set to 10 steps, and sampling time are set to 0.1 s. It can be observed that the proposed controller reaches a comparable level of computational efficiency compared to classic kinematic MPC controller. The reason for this is that the proposed controller is also based on kinematic vehicle model. Thus, both kinematic MPC have almost the same computing efficiency in solving the problem of path tracking. In addition, it is obvious that the dynamic MPC controller has the worst computational efficiency compared to others.

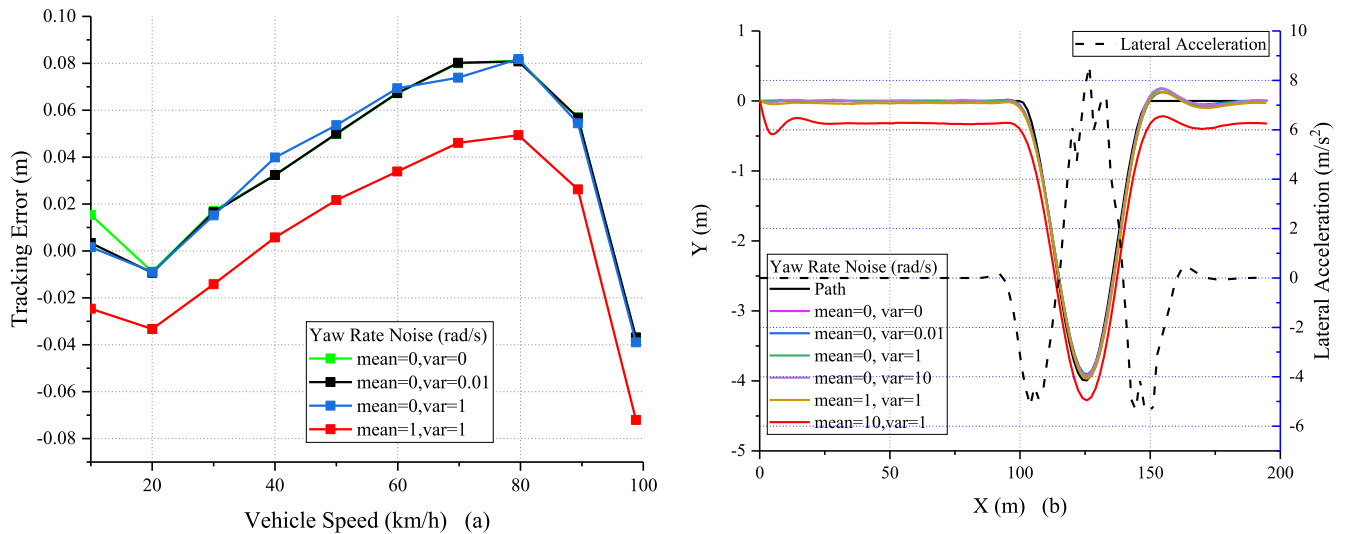


FIGURE 10. The robustness against the measurement error of the yaw rate sensor: a) steady-state, b) transient-state at the limits of handling (60 km/h).

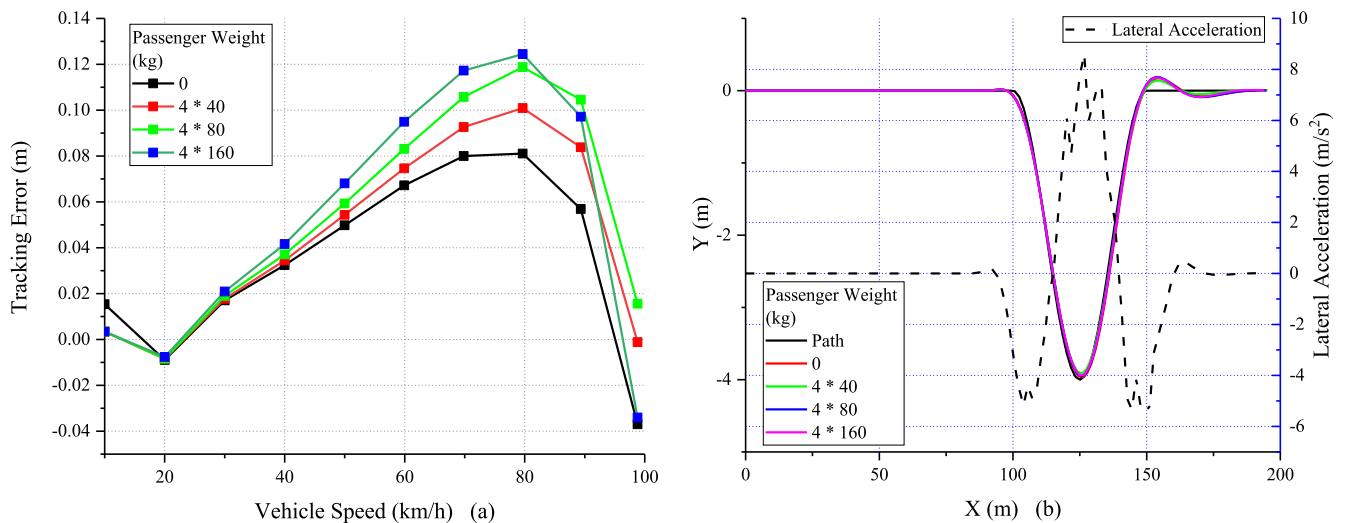


FIGURE 11. Robustness against parameters uncertainties: vehicle mass uncertainties. a) steady-state, b) transient-state at the limits of handling (60 km/h).

V. FIELD TEST

A. VEHICLE PLATFORM

The proposed cascaded MPC-PID with sideslip compensator was implemented on an autonomous electric vehicle—Dongfeng A60EV, as shown in Figure 14. A real-time kinematic (RTK) positioning system and inertial measurement unit RT3002 were used to obtain global vehicle states. The controller was implemented in C++ under Ubuntu and Robot Operating System with an intel i7-6700k processor and operates at 50 Hz. The target vehicle longitudinal speed was followed by a PID controller. Because of space limitations of experimental field, only a circular path with a radius of 14 m was used for experimental validation. Although it does not cover all test cases to verify the proposed approach, especially lacking of high speed scenarios, it is

adequate to validate the robustness against measurement error of the yaw rate sensor and time lag, which are the main concern about validation on the premise of the aforementioned simulations.

B. EXPERIMENTAL RESULTS

Figure 15 presents the experimental results for following a circular path on concrete road surface. The vehicle speed varies from 10 km/h to 32 km/h in consideration of safety. Note that although the vehicle speed is not very high in this field test, the resulting maximum lateral acceleration could be aggressive (5.84 m/s²), due to the small road radius. It can be found that the proposed controller restricts the lateral tracking error into a range of 0.08 m, which denotes remarkable tracking accuracy and is identical with

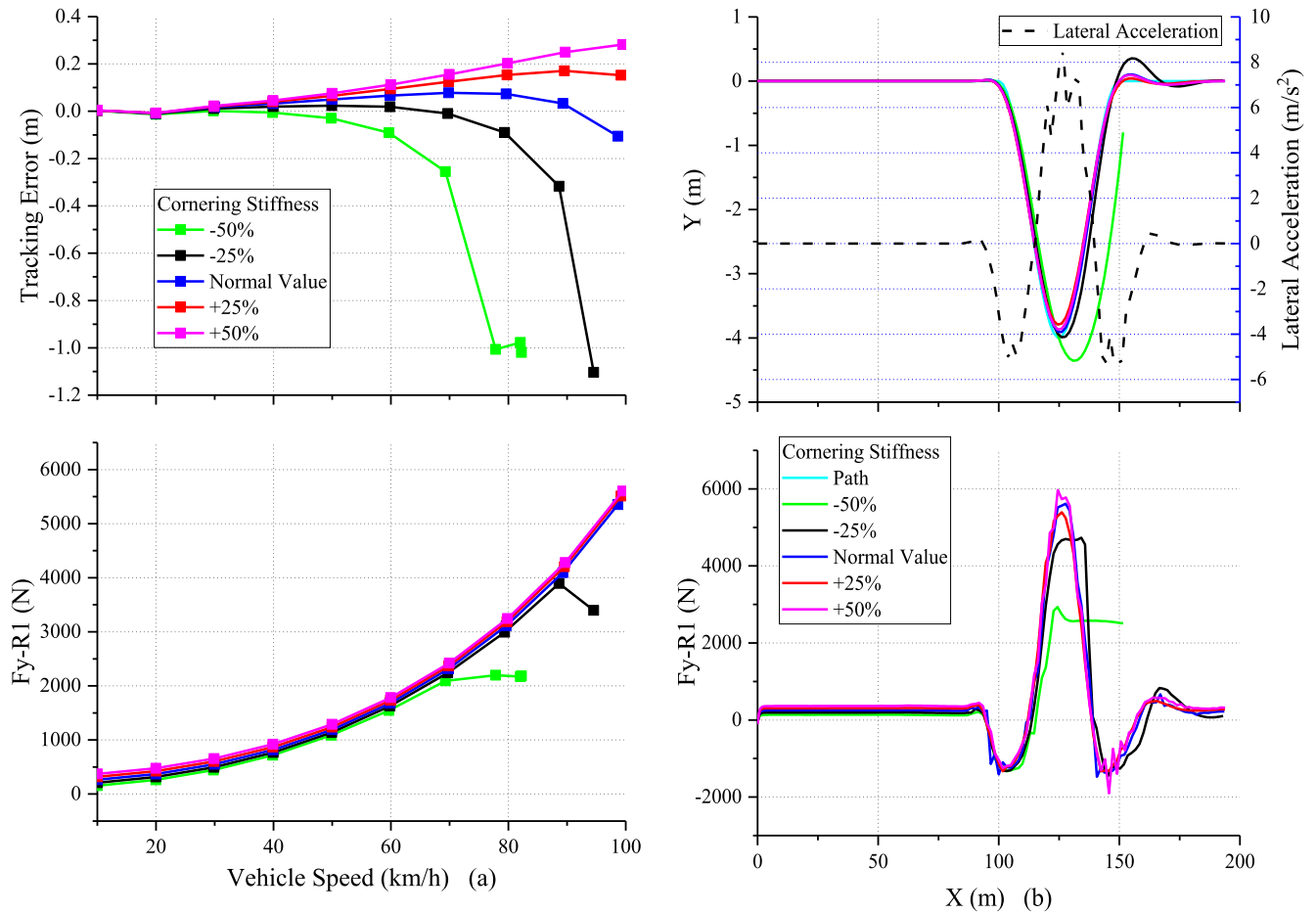


FIGURE 12. Robustness against parameters uncertainties: cornering stiffness uncertainties. a) steady-state test, Fy-R1 denotes the lateral forces of right front tire. b) transient-state at the limits of handling (60 km/h).

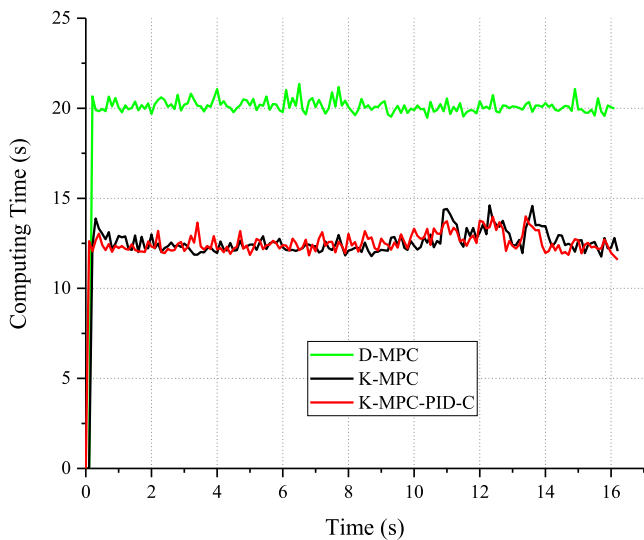


FIGURE 13. Comparison of computing time with the same MPC configurations that both the prediction horizon and control horizon are set to 10 steps, and sampling time are set to 0.1 s.



FIGURE 14. Dongfeng A60EV used for field test.

by MPC loop is followed well by the real yaw rate and both yaw rate change smoothly, which confirms the outstanding prediction performance of MPC control with sideslip compensation and the robustness under real inertial measurement unit. In short, this experimental results indicate that in the real world the proposed controller is capable of providing comparably good tracking performance with simulation.

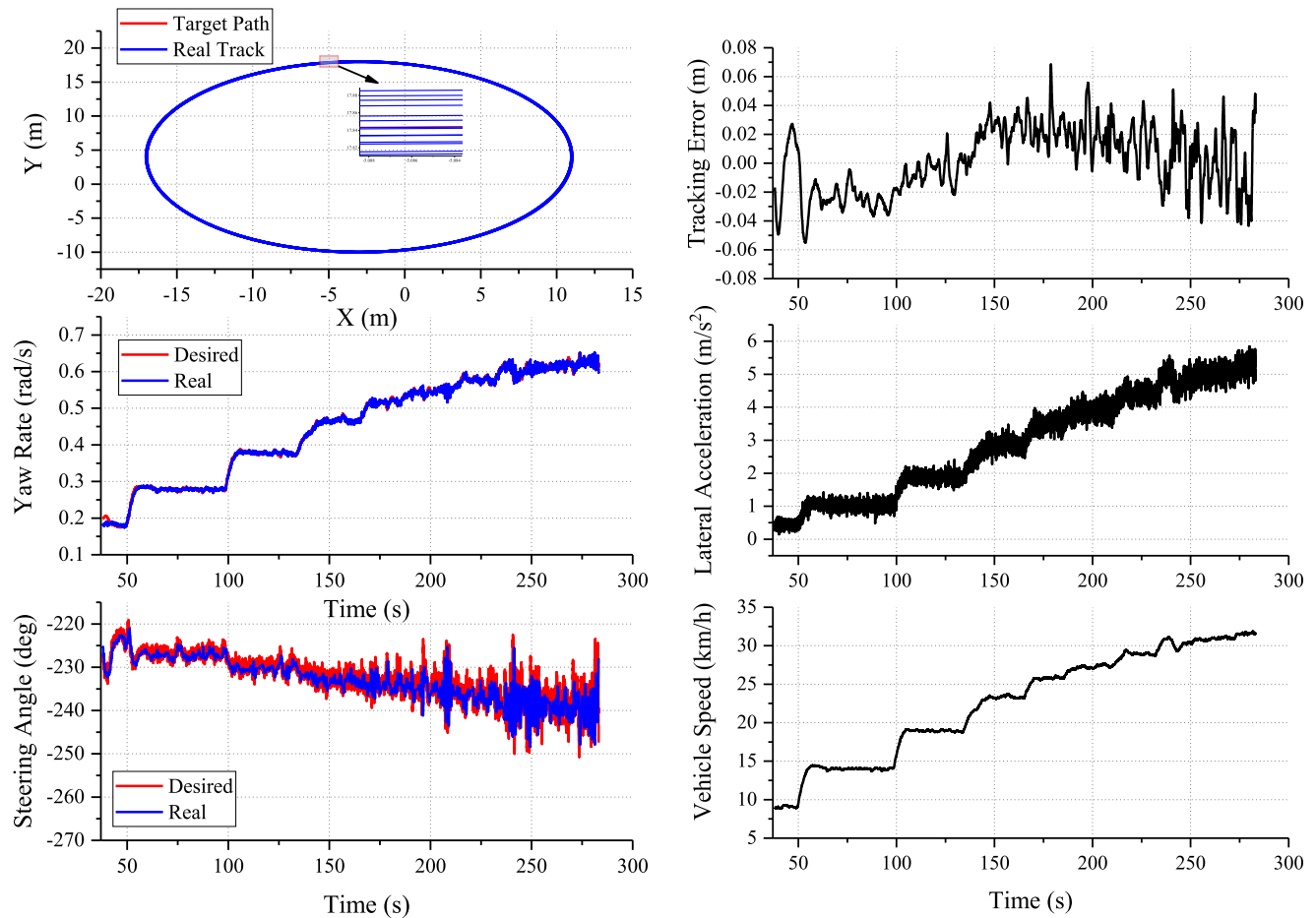


FIGURE 15. Experimental results for following a circular path with a radius of 14 m.

VI. CONCLUSION

This paper describes the design of a cascaded kinematic MPC-PID controller with vehicle sideslip compensation for path tracking of autonomous vehicles. A kinematic MPC based on yaw rate is derived to tackle the disturbances of the upcoming road curvature at various speeds. Subsequently, in consideration of the kinematic model mismatch at high speed, a novel vehicle sideslip compensator is proposed to correct model prediction and is integrated into the kinematic model. Note that the MPC control loop outputs desired yaw rate rather than steering angle compared to classic MPC controller for path tracking. Then, a PID control is designed to follow the reference yaw rate, which takes full advantage of the feedback of yaw rate to reject uncertainties and modeling errors.

The proposed controller performances involving steady-state and transient response, robustness, and computing efficiency were evaluated on Carsim/Matlab joint simulation environment. The simulation results demonstrate that the proposed controller is successful to resolve the dilemma that kinematic MPC only works well at low speed while dynamic MPC has poor computational efficiency and gets worse at

low speed, with the improvement for path tracking that the tracking errors are guaranteed less than 0.16 m, ranging from low speed to high speed even at the limits of handling. In addition, due to the utilization of kinematic model, the proposed control method reaches a comparable level of computational efficiency compared to classic kinematic MPC. Furthermore, simulation and field experiments conducted with the A60EV autonomous vehicle validate the robustness against sensor disturbances and time lag. Lastly, this research has also confirmed that

1) the developed vehicle sideslip compensator is sufficient to capture steer dynamics and mitigate the effect of vehicle sideslip angle in the proposed control architecture. This finding may be incorporated into other control law based on the feedback of yaw rate to improve path tracking.

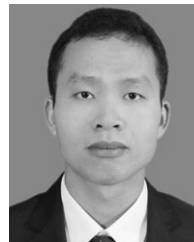
2) As for classic MPC controller for path tracking, the controller cannot trigger a switch from kinematic MPC to linear dynamic MPC just according to the increase of vehicle speed, because their tracking performances depend on not only vehicle speed, but also road curvature and the resulting lateral acceleration, consequently, which makes it difficult to combine the kinematic MPC and dynamic MPC for improving

tracking performance. The above weakness of classic MPC for path tracking highlights the contribution of the proposed control law.

Future work will focus on the implementation of the proposed control method with embedded platform such as NVIDIA Nano Kit.

REFERENCES

- [1] N. R. Kapania and J. C. Gerdes, "Design of a feedback-feedforward steering controller for accurate path tracking and stability at the limits of handling," *Vehicle Syst. Dyn.*, vol. 53, no. 12, pp. 1687–1704, Dec. 2015.
- [2] G. Tagne, R. Tajj, and A. Charara, "Design and comparison of robust nonlinear controllers for the lateral dynamics of intelligent vehicles," *IEEE Trans. Intell. Transp. Syst.*, vol. 17, no. 3, pp. 796–809, Mar. 2016.
- [3] M. T. Emirler, İ. M. C. Uygan, B. A. Güvenç, and L. Güvenç, "Robust PID steering control in parameter space for highly automated driving," *Int. J. Veh. Technol.*, vol. 2014, Nov. 2014, Art. no. 259465.
- [4] R. Marino, S. Scalzi, G. Orlando, and M. Netto, "A nested PID steering control for lane keeping in vision based autonomous vehicles," in *Proc. Amer. Control Conf. (ACC)*, 2009, pp. 2885–2890.
- [5] B. Mashadi, M. Mahmoudi-Kaleybar, P. Ahmadizadeh, and A. Oveisi, "A path-following driver/vehicle model with optimized lateral dynamic controller," *Latin Amer. J. Solids Struct.*, vol. 11, no. 4, pp. 613–630, Aug. 2014.
- [6] M. Buehler, K. Iagnemma, and S. Singh, *The 2005 DARPA Grand Challenge: The Great Robot Race*, vol. 36. Berlin, Germany: Springer, 2007.
- [7] R. Liu and J. Duan, "A path tracking algorithm of intelligent vehicle by preview strategy," in *Proc. 32nd Chin. Control Conf.*, 2013, pp. 5630–5635.
- [8] Y. Shan, W. Yang, C. Chen, J. Zhou, L. Zheng, and B. Li, "CF-pursuit: A pursuit method with a clothoid fitting and a fuzzy controller for autonomous vehicles," *Int. J. Adv. Robot. Syst.*, vol. 12, no. 9, p. 134, Sep. 2015.
- [9] N. H. Amer, H. Zamzuri, K. Hudha, and Z. A. Kadir, "Modelling and control strategies in path tracking control for autonomous ground vehicles: A review of state of the art and challenges," *J. Intell. Robot. Syst.*, vol. 86, no. 2, pp. 225–254, May 2017.
- [10] T. Ming, W. Deng, S. Zhang, and B. Zhu, "MPC-based trajectory tracking control for intelligent vehicles," SAE, Warrendale, PA, USA, Tech. Rep. 0148-7191, 2016.
- [11] B. Zhang, C. Zong, G. Chen, and B. Zhang, "Electrical vehicle path tracking based model predictive control with a Laguerre function and exponential weight," *IEEE Access*, vol. 7, pp. 17082–17097, 2019.
- [12] C. Shen, H. Guo, F. Liu, and H. Chen, "MPC-based path tracking controller design for autonomous ground vehicles," in *Proc. 36th Chin. Control Conf. (CCC)*, 2017, pp. 9584–9589.
- [13] H. Wang, B. Liu, X. Ping, and Q. An, "Path tracking control for autonomous vehicles based on an improved MPC," *IEEE Access*, vol. 7, pp. 161064–161073, 2019.
- [14] C. Sun, X. Zhang, Q. Zhou, and Y. Tian, "A model predictive controller with switched tracking error for autonomous vehicle path tracking," *IEEE Access*, vol. 7, pp. 53103–53114, 2019.
- [15] M. Babu, R. R. Theerthala, A. K. Singh, B. P. Baladhurgesh, B. Gopalakrishnan, K. M. Krishna, and S. Medasani, "Model predictive control for autonomous driving considering actuator dynamics," in *Proc. Amer. Control Conf. (ACC)*, Jul. 2019, pp. 1983–1989.
- [16] J. Cai, H. Jiang, L. Chen, J. Liu, Y. Cai, and J. Wang, "Implementation and development of a trajectory tracking control system for intelligent vehicle," *J. Intell. Robot. Syst.*, vol. 94, no. 1, pp. 251–264, Apr. 2019.
- [17] S. Xu and H. Peng, "Design, analysis, and experiments of preview path tracking control for autonomous vehicles," *IEEE Trans. Intell. Transp. Syst.*, vol. 21, no. 1, pp. 48–58, Jan. 2020.
- [18] J. Bechtloff, L. Koenig, and R. Isermann, "Cornering stiffness and sideslip angle estimation for integrated vehicle dynamics control," *IFAC-PapersOnLine*, vol. 49, no. 11, pp. 297–304, 2016.
- [19] H. Pacejka, *Tire and Vehicle Dynamics*. Amsterdam, The Netherlands: Elsevier, 2005.
- [20] C. Zhang, J. Hu, J. Qiu, W. Yang, H. Sun, and Q. Chen, "A novel fuzzy observer-based steering control approach for path tracking in autonomous vehicles," *IEEE Trans. Fuzzy Syst.*, vol. 27, pp. 278–290, Jul. 2019.
- [21] A. Carvalho, Y. Gao, S. Lefevre, and F. Borrelli, "Stochastic predictive control of autonomous vehicles in uncertain environments," in *Proc. 12th Int. Symp. Adv. Vehicle Control*, 2014, pp. 712–719.
- [22] M. Bojarski, D. Del Testa, D. Dworakowski, B. Firner, B. Flepp, P. Goyal, L. D. Jackel, M. Monfort, U. Müller, J. Zhang, X. Zhang, J. Zhao, and K. Zieba, "End to end learning for self-driving cars," 2016, *arXiv:1604.07316*. [Online]. Available: <https://arxiv.org/abs/1604.07316>
- [23] N. R. Kapania and J. C. Gerdes, "Path tracking of highly dynamic autonomous vehicle trajectories via iterative learning control," in *Proc. Amer. Control Conf. (ACC)*, Jul. 2015, pp. 2753–2758.
- [24] S. Liu, Z. Hou, T. Tian, Z. Deng, and Z. Li, "A novel dual successive projection-based model-free adaptive control method and application to an autonomous car," *IEEE Trans. Neural Netw. Learn. Syst.*, vol. 30, no. 11, pp. 3444–3457, Nov. 2019.
- [25] S. Dixit, S. Fallah, U. Montanaro, M. Dianati, A. Stevens, F. Mccullough, and A. Mouzakitis, "Trajectory planning and tracking for autonomous overtaking: State-of-the-art and future prospects," *Annu. Rev. Control*, vol. 45, pp. 76–86, Jan. 2018.
- [26] J. Ackermann, J. Guldner, W. Sienel, R. Steinhauser, and V. I. Utkin, "Linear and nonlinear controller design for robust automatic steering," *IEEE Trans. Control Syst. Technol.*, vol. 3, no. 1, pp. 132–143, Mar. 1995.
- [27] J. Guo, Y. Luo, K. Li, and Y. Dai, "Coordinated path-following and direct yaw-moment control of autonomous electric vehicles with sideslip angle estimation," *Mech. Syst. Signal Process.*, vol. 105, pp. 183–199, May 2018.
- [28] R. Attia, R. Orjuela, and M. Basset, "Combined longitudinal and lateral control for automated vehicle guidance," *Vehicle Syst. Dyn.*, vol. 52, no. 2, pp. 261–279, Feb. 2014.
- [29] J. Zhao and A. E. Kamel, "Integrated longitudinal and lateral control system design for autonomous vehicles," *IFAC Proc. Volumes*, vol. 42, no. 19, pp. 496–501, 2009.
- [30] J. Kong, M. Pfeiffer, G. Schildbach, and F. Borrelli, "Kinematic and dynamic vehicle models for autonomous driving control design," in *Proc. IEEE Intell. Vehicles Symp. (IV)*, Jun. 2015, pp. 1094–1099.
- [31] L. T. Biegler, A. M. Cervantes, and A. Wächter, "Advances in simultaneous strategies for dynamic process optimization," *Chem. Eng. Sci.*, vol. 57, no. 4, pp. 575–593, Feb. 2002.
- [32] Z. Chu, N. Chen, N. Zhang, and G. Li, "Path-tracking for autonomous vehicles with on-line estimation of axle cornering stiffnesses," in *Proc. Chin. Control Conf. (CCC)*, Jul. 2019, pp. 6651–6657.
- [33] B. L. Boada, M. J. L. Boada, and H. Zhang, "Sensor fusion based on a dual Kalman filter for estimation of road irregularities and vehicle mass under static and dynamic conditions," *IEEE/ASME Trans. Mechatronics*, vol. 24, no. 3, pp. 1075–1086, Jun. 2019.



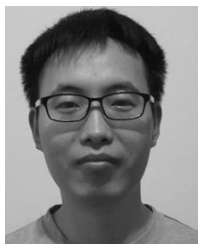
LUQI TANG received the B.S. degree in thermal energy and power engineering and the M.S. degree in power machinery and engineering from the School of Automotive Engineering, Wuhan University of Technology, China, in 2012 and 2015, respectively, where he is currently pursuing the Ph.D. degree in automotive engineering. His research interests include decision making, vehicle dynamics, and control for autonomous vehicles.



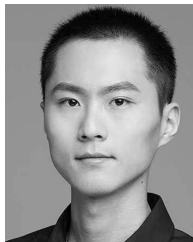
FUWU YAN is currently the Dean of the School of Automotive Engineering, Wuhan University of Technology, where he is also a Chief Professor of automotive engineering. He is also the Director of the Hubei Research Center for New Energy & Intelligent Connected Vehicle. His research interests include electrification of vehicles, powertrain control, and autonomous vehicles.



BIN ZOU received the Ph.D. degree in power machinery and engineering from the Wuhan University of Technology, Wuhan, China, in 2013. He is currently an Associate Professor with the School of Automotive Engineering, Wuhan University of Technology. His current research interests include automobile electronic control and autonomous vehicles.



KEWEI WANG received the B.S. degree in automotive engineering from the School of Automotive Engineering, Wuhan University of Technology, China, in 2013, where he is currently pursuing the Ph.D. degree in automotive engineering. His research interests include environment perception and multisensor fusion in autonomous driving.



CHEN LV (Member, IEEE) received the Ph.D. degree from the Department of Automotive Engineering, Tsinghua University, Beijing, China, in 2016. He was a Research Fellow with the Advanced Vehicle Engineering Center, Cranfield University, Cranfield, U.K., from 2016 to 2018, and a joint Ph.D. Researcher with the Electrical Engineering and Computer Sciences, University of California, Berkeley, CA, USA, from 2014 to 2015. He is currently an Assistant Professor with the School of Mechanical and Aerospace Engineering, Nanyang Technological University, Singapore. His research interests include cyber-physical systems and advanced vehicle control and intelligence, in which he has contributed more than 60 articles and obtained 11 granted China patents. Dr. Lv was a recipient of the Highly Commended Paper Award of IMechE, U.K., in 2012, the NSK Outstanding Mechanical Engineering Paper Award, in 2014, the China SAE Outstanding Paper Award, in 2015, the First Class Award of China Automotive Industry Scientific and Technological Invention, in 2015, and the Tsinghua University Outstanding Doctoral Thesis Award, in 2016. He serves as a Guest Editor for the IEEE/ASME TRANSACTIONS ON MECHATRONICS and the IEEE TRANSACTIONS ON INDUSTRIAL INFORMATICS, and an Associate Editor for the *International Journal of Electric and Hybrid Vehicles* and the *International Journal of Vehicle Systems Modelling and Testing*.

• • •